

# Site-Specific Response Spectra: 2<sup>nd</sup> District of Cagayan de Oro City, Philippines

Israel A. Baguhin\* and Jerson N. Orejudos  
College of Engineering and Technology  
Mindanao State University – Iligan Institute of Technology  
Iligan City, 9200 Philippines  
\*israel.baguhin@ustp.edu.ph

Date received: August 28, 2019

Revision accepted: February 5, 2020

---

## Abstract

*Building codes are updated advertently to address the catastrophic effect of earthquakes. One way of mitigating it is the development of a site-specific response spectrum. In the Philippines, the National Structural Code of the Philippines (NPSC) is the recognized National Building Code adopting the 1997 Uniform Building Code (UBC). The NSCP uses the 10% probability of exceedance in a 50-year period with a return period of 475 years. In this study, site-specific response spectra were developed in the 2<sup>nd</sup> District of Cagayan de Oro City using a 300-km radius, with coordinates of 8.235° (latitude) and 124.024° (longitude) as the center point of the study area, using the same probability of exceedance in a 50-year period. Historical earthquake catalogs were gathered from the United States Geological Survey and the Department of Science and Technology – Philippine Institute of Volcanology and Seismology. Local soil condition was assimilated in the study to take into account the soil response. Finally, site-specific response spectra were developed using the probabilistic seismic hazard analysis where substantial results are achieved, i.e., the UBC 1997 design response spectrum is remarkably high in spectral acceleration values at 0.01, 0.20, 1.0, 2.0, 3.0, 4.0 and 5.0 s at 0.44, 1.1, 1.1, 0.7, 0.36, 0.26 and 0.20 g compared to the maximum site-specific response spectra of the study area of the same period at 0.39, 0.92, 0.23, 0.10, 0.07, 0.05 and 0.04 g spectral accelerations, respectively.*

**Keywords:** earthquake, local site condition, probabilistic seismic hazard analysis, shear-wave velocity, ground motion prediction equation

---

## 1. Introduction

Modern structures nowadays are meticulously designed due to the occurrence of earthquakes. An earthquake is a sudden and violent shaking of the ground as a result of movement within the earth's crust, causing great destruction to lives and properties. It is an unpredictable and catastrophic phenomenon that

may happen anytime throughout the globe, giving rise to anxiety in terms of safety and comfort in our homes.

During an earthquake, building structures would shake and move horizontally and vertically. If the building is overly reinforced, it would suddenly collapse without giving any warning to its occupants which results in casualties. However, if the building structure is designed based on specific data, i.e., not overly reinforced, it would not abruptly collapse giving ample time for its occupants to stay away from danger. To protect and assure the public of security, building codes have been developed and updated intently, taking into consideration the earthquake ground shaking in the design and requiring standards in building construction.

Presently, the Philippine government uses the National Structural Code of the Philippines (NSCP) (2015) adopting the 1997 Uniform Building Code (UBC). The UBC (1997) design response spectrum is a generalized response spectrum, which is not site-specific. It uses the deterministic approach in constructing the response spectrum where only the maximum earthquake magnitude is being considered (Sil and Sitharam, 2016). Seismic parameters are taken from the other country, i.e., from the 1994 Northridge record in San Fernando Valley, Los Angeles, California, USA and soil effects are just an estimation depending on the near-source factors  $N_a$  and  $N_v$  (NSCP, 2015).

In this study, site-specific response spectra were developed using representative and specific data from the 2<sup>nd</sup> District of Cagayan de Oro City, Philippines (Figure 1) incorporating actual soil conditions (Dungca and Macaraeg, 2016). Earthquake seismic sources and magnitudes within the 300-km radius, with coordinates of  $8.235^\circ$  (latitude) and  $124.024^\circ$  (longitude) as the center point, were considered using the Probabilistic Seismic Hazard Assessment (PSHA) (Anbazhagan *et al.*, 2017). The PSHA approach scrutinizes all earthquake magnitudes above 4.0 and calculates its probabilities of occurrence in each seismic source. The developed ground surface site-specific response spectra are then compared to that of the UBC 1997 design response spectrum in terms of spectral acceleration values at 0.01, 0.20, 1.0, 2.0, 3.0, 4.0 and 5.0 s time periods where the ground motion representation is a 10% probability of being exceeded in 50 years with a return period of 475 years (NSCP, 2015).

## 2. Methodology

### 2.1 Study Area

The scope of the study area included 56 sites in the 2<sup>nd</sup> District of Cagayan de Oro City as shown in Figure 1 namely, Agusan, Balubal, Bugo, Camaman-an, Consolacion, Cugman, FS Catanico, Gusa, Indahag, Lapasan, Macabalan, Macasandig, Nazareth, Puerto, Puntod, Tablon and Barangays 1 to 40.

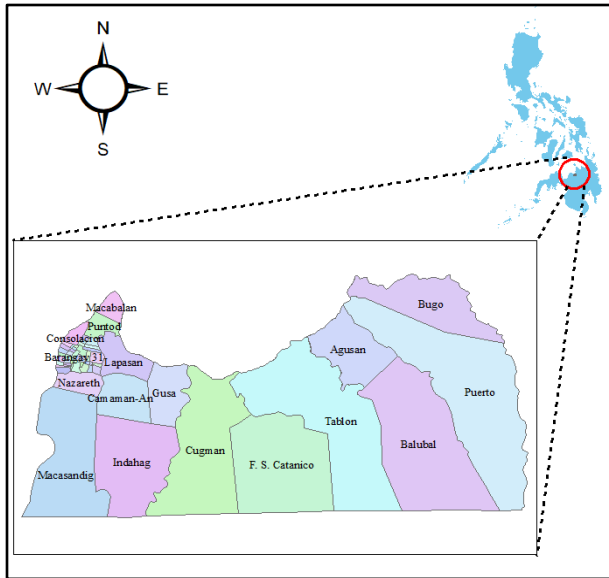


Figure 1. The study area

### 2.2 Earthquake Catalogues

Earthquake catalogs were gathered from the United States Geological Survey (USGS) website and the Department of Science and Technology – Philippine Institute of Volcanology and Seismology (DOST-PHIVOLCS) in Metro Manila, Philippines.

### 2.3 Homogenization of Earthquake Catalogues

Earthquake catalogs were homogenized (Ahmad, 2016), converting every earthquake magnitude such as surface-wave magnitude ( $M_s$ ), body-wave magnitude ( $M_b$ ) and local magnitude ( $M_L$ ) to moment magnitude ( $M_w$ ) as shown in Table 1.

Table 1. Correlation of earthquake magnitudes to  $M_w$

Item	Relationship Type	Conversion
1	$M_w$ and $M_s \leq 6.2$	$M_w = 0.535M_s + 2.69$
2	$M_w$ and $M_s > 6.2$	$M_w = 0.895M_s + 0.53$
3	$M_w$ and $M_b$	$M_w = M_b + 0.103$
4	$M_w$ and $M_L$	$M_w = 0.878M_L + 0.838$

### 2.4 ZMAP Software

The ZMAP software (Ahmad, 2016) was used for de-clustering and removal of foreshocks and aftershocks in earthquake catalogs using Reasenberg Method (Teng and Baker, 2019). The software is also used to determine earthquake seismic parameters “a” and “b” in every seismic source using the average value and maximum sampling radius of 60 km. The “a” and “b” values indicate the seismicity rate and the ratio of small to large earthquakes. Equations 1 and 2 were used to calculate the corresponding values of  $\alpha$  and  $\beta$ , and subsequently, the mean annual exceedance (Equation 3). The values of  $M_0$  and  $M_{max}$  were determined from the ZMAP software.

$$\alpha = a \times \ln 10 \tag{1}$$

$$\beta = b \times \ln 10 \tag{2}$$

$$\lambda_{\alpha,\beta,M_0,M_{max}} = e^{(\alpha-\beta M_0)} [e^{(-\beta(M-M_0))} - e^{(-\beta(M_{max}-M_0))}] \left[ \frac{1}{1 - e^{(-\beta(M_{max}-M_0))}} \right] \tag{3}$$

### 2.5 Completeness Analysis of Earthquake Catalogues

The de-clustered earthquake catalog was analyzed for completeness using the Stepp Method (Stepp, 2001) and Cumulative Visual (CUVI) (Ahmad, 2016). In the Stepp method (Salamat and Zare, 2015), earthquake records in the catalog are grouped into different magnitude class. Each magnitude is modeled as a point process in time where the mean rate of occurrence of earthquakes in a magnitude range is established. It is assumed that the earthquake sequence follows a Poisson’s distribution for obtaining an accurate estimate of the variance of the sample mean. Let  $k_1, k_2, \dots, k_n$  be the number of events per unit time interval, then the unbiased estimate of the mean per unit interval is given by Equation 4.

$$\lambda = \frac{1}{n} \sum_{i=1}^n k_i \tag{4}$$

where  $n$  is the unit time interval and its variance is  $\sigma_\lambda^2 = \frac{\lambda}{n}$ . The standard deviation is  $\sigma_\lambda = \frac{1}{\sqrt{n}}$  where the process is assumed to be stationary; during this period, the mean rate of occurrence in a magnitude class is constant. The deviation of the standard deviation of the estimate of the mean from the tangent line indicates the length up to which a particular magnitude range is complete. On the other hand, in the CUVI method, completeness starts at the earliest time when the slope of the cumulative fitting curve is approximately a straight line (Ahmad, 2016).

### *2.6 Identifying Earthquake Sources*

In this study, 19 line seismic sources were identified as capable of producing ruinous ground motions namely, (1) Tagoloan River Fault, (2) Cabanglasan Fault, (3) Central Mindanao Fault, (4) Davao River Fault, (5) Philippine Fault Zone (PFZ) Mati Fault, (6) PFZ Lianga Fault, (7) PFZ Eastern Mindanao Fault, (8) Tangbulan Fault, (9) Mindanao Fault (MF) Daguma Extension, (10) Lanao Fault System, (11) MF Western Mindanao Extension, (12) Zamboanga Fault System, (13) East Bohol Fault, (14) Central Negros Fault, (15) Cebu Lineament, (16) PFZ Central Leyte Fault, (17) Philippine Trench, (18) Sulu Trench and (19) Cotabato Trench.

### *2.7 Identifying Earthquake Magnitudes*

Seismic sources can produce earthquakes of varying magnitudes following a particular distribution known as Gutenberg-Richter recurrence law using Equation 5.

$$\log \lambda_m = a - bm \tag{5}$$

Where  $\lambda_m$  is the rate of earthquakes with magnitudes greater than  $m_j$ . Equation 6 was used to calculate the Cumulative Distribution Function (CDF).

$$\begin{aligned} CDF = F_M(m) &= P(M \leq m | M > m_{\min}) \\ &= 1 - 10^{-b(m - m_{\min})}, m > m_{\min} \end{aligned} \tag{6}$$

If the maximum magnitude that a given source can produce is already known, Equation 6 become Equation 7.

$$CDF = \frac{1 - 10^{-b(m - m_{\min})}}{1 - 10^{-b(m_{\max} - m_{\min})}}, m_{\min} < m < m_{\max} \quad (7)$$

The probabilities of occurrence were then computed using Equation 8.

$$P(M = m_j) = F_M(m_{j+1}) - F_M(m_j) \quad (8)$$

Where  $m_j$  are ordered discrete set of magnitudes so that  $m_j < m_{j+1}$

### 2.8 Soil Test Reports

Geotechnical soil test reports were gathered from the Department of Public Works and Highways (DPWH) in Bulua and Macabalan, Cagayan de Oro City, Philippines. The SPT-N values of 95 boreholes in the 2<sup>nd</sup> District of Cagayan de Oro City were correlated (Akin *et al.*, 2011; Boore, 2011) to predict the average upper 30-m shear-wave velocity of the soil using Equations 9 and 10.

$$V_s = 59.44 N^{0.109} Z^{0.426} \quad (9)$$

$$\log V_{S30} = c_o + c_1 \log V_{S_z} + c_2 (\log V_{S_z})^2 \quad (10)$$

The coefficients and standard deviation of the residuals to the fit ( $\sigma_{RES}$ ) are shown in Table 2.

### 2.9 Ground Motion Prediction Equation (GMPE)

In this study, the attenuation equation for soil sites (Atkinson and Boore, 2006) was used to predict the ground surface response spectra in the 2<sup>nd</sup> District of Cagayan de Oro City since the study area is a broad and coastal alluvial plain (Cagayan de Oro City Planning and Development Office, 2015) utilizing the R-CRISIS 2015 software (Ordaz and Salgado-Galvez, 2017).

**Table 2. Coefficients relating  $\log V_{s30}$  and  $\log V_{sz}$  regardless of site class**

Depth, z	$c_0$	$c_1$	$c_2$	$\sigma_{RES}$
5	0.2046	1.318	-0.1174	0.119
6	-0.06072	1.482	-0.1423	0.111
7	-0.2744	1.607	-0.1600	0.103
8	-0.3723	1.649	-0.1634	0.097
9	-0.4941	1.707	-0.1692	0.090
10	-0.5438	1.715	-0.1667	0.084
11	-0.6006	1.727	-0.1649	0.078
12	-0.6082	1.707	-0.1576	0.072
13	-0.6322	1.698	-0.1524	0.067
14	-0.6118	1.659	-0.1421	0.062
15	-0.5780	1.611	-0.1303	0.056
16	-0.5430	1.565	-0.1193	0.052
17	-0.5282	1.535	-0.1115	0.047
18	-0.4960	1.494	-0.1020	0.043
19	-0.4552	1.447	-0.09156	0.038
20	-0.4059	1.396	-0.08064	0.035
21	-0.3827	1.365	-0.07338	0.030
22	-0.3531	1.331	-0.06585	0.027
23	-0.3158	1.291	-0.05751	0.023
24	-0.2736	1.250	-0.04896	0.019
25	-0.2227	1.202	-0.03943	0.016
26	-0.1768	1.159	-0.03087	0.013
27	-0.1349	1.120	-0.02310	0.009
28	-0.09038	1.080	-0.01527	0.006
29	-0.04612	1.040	-0.007618	0.003

### 2.10 ArcGIS Software

The ArcGIS software was used in interpolating the estimated average shear-wave velocities in the upper 30-m depth of soil utilizing the empirical Bayesian Kriging Method. The shapefile was then converted to a  $V_{s30}$  .grd file for analysis in R-CRISIS 2015 software for site effects consideration.

### 2.11 R-CRISIS Software

The R-CRISIS 2015 was used in developing the site-specific response spectra incorporating all data and files namely, map file, city file, grid of site, seismic source geometry, seismic source seismicity, attenuation equation, spectral ordinates, global parameters and site effects.

### **3. Results and Discussion**

#### *3.1 De-clustering of Earthquake Catalogue Using the ZMAP Software*

The homogenized earthquake catalog consists of 8,957 earthquake moment magnitude events. After de-clustering using the Reasenberg Method in the ZMAP software, the earthquake catalog was reduced to 6,804 moment magnitude events, removing earthquake foreshocks and aftershocks as shown in Figure 2.

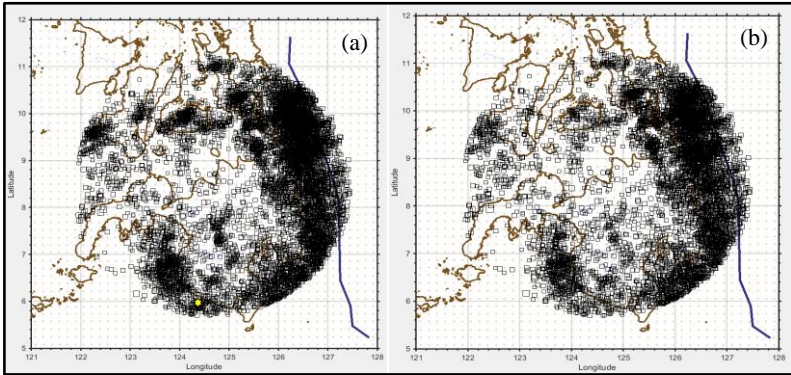


Figure 2. Seismicity of the study area using a 300-km radius before de-clustering (a) and after de-clustering (b)

Figures 2a and 2b show the earthquake catalog within the 300-km radius, with coordinates of 8.235° (latitude) and 124.024° (longitude) as the center point of the study area, containing 8957 and 6804-moment magnitude earthquake events before (original) and after de-clustering. The de-clustering was done on the earthquake catalogue so that only earthquake mainshocks were considered and analyzed in the PSHA method.

#### *3.2 Determination of Seismic Parameters “a” and “b”*

##### *Using the ZMAP Software*

After de-clustering the earthquake catalog, the ZMAP software was used for calculating b-value parameter for magnitude completeness as shown in Figure 3.

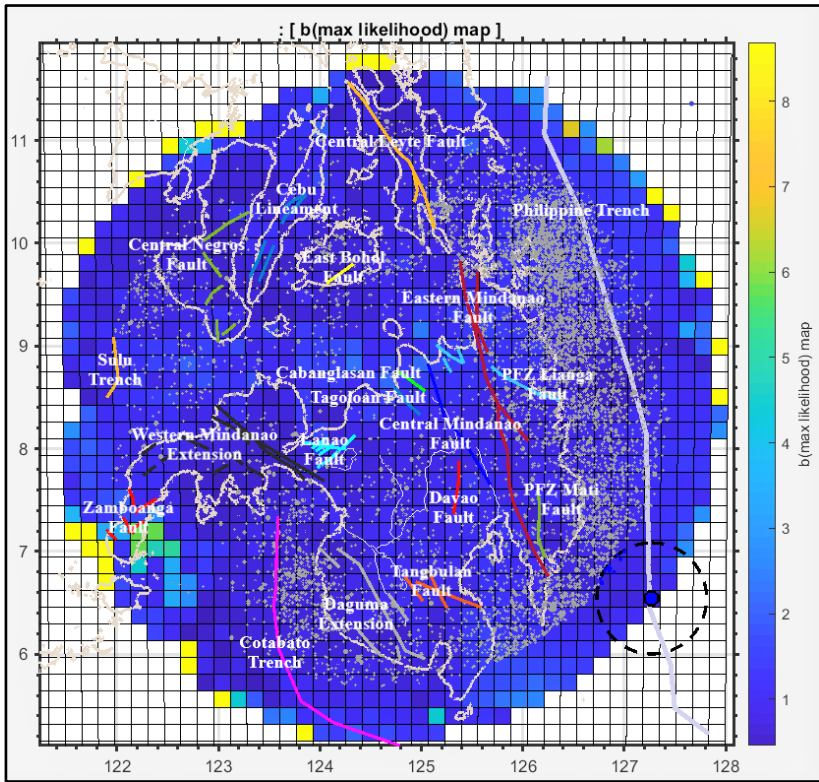


Figure 3. Determination of seismic parameter “b” in all seismic sources using MLE

Figure 3 exemplifies the Maximum Likelihood Estimation (MLE) of seismic parameter “b” using  $0.05^\circ \times 0.05^\circ$  grid cells, incorporating all fault lines and earthquake moment magnitudes within the 300-km radius of the study area. Numerical values in each cell of every line seismic source were taken. The average value was then calculated in every line seismic source (as shown in Table 3). Using a sampling radius of 60-km, the seismic parameter “a” was obtained and the corresponding values of  $\alpha$ ,  $\beta$  and  $\lambda_{\alpha,\beta,M_o,M_{max}}$  were then computed using Equations 1, 2 and 3 as summarized in Table 3.

In Table 3, a-value and b-value are the seismicity and the ratio of small to large moment magnitude earthquakes. The bigger the a-value, the higher is the seismicity of the area; when the b-value is more than 1.0, small moment magnitude earthquakes occur more often than the larger ones. In the table, small moment magnitude earthquakes were dominant over large moment magnitude earthquakes in Tagoloan River, Cabanglasan, Central Mindanao,

Table 3. Seismic values of a, b,  $\alpha$ ,  $\beta$  and  $\lambda_{\alpha,\beta,M_0,M_{max}}$  in all seismic sources

Seismic Sources/Faults	a	b	$\alpha$	$\beta$	$\lambda_{\alpha,\beta,M_0,M_{max}}$
Tagoloan River	7.36	1.17	16.95	2.69	18.9
Cabanglasan	8.23	1.37	19.00	3.15	17.5
Central Mindanao	7.08	1.08	16.30	2.49	47.9
Davao River	6.86	1.04	15.80	2.39	58.1
PFZ Mati	7.02	0.97	16.16	2.23	147.9
PFZ Lianga	8.56	1.28	19.71	2.95	107.6
PFZ Eastern Mindanao	7.49	1.07	17.25	2.46	138.0
Tangbunan	6.80	0.97	15.66	2.23	111.4
MF Daguma	6.11	0.83	14.07	1.91	110.4
Lanao	6.16	0.89	14.18	2.05	27.7
MF Western Mindanao Ext.	5.91	0.86	13.61	1.98	33.4
Zamboanga	6.25	0.99	14.39	2.28	10.1
East Bohol	5.41	0.73	12.46	1.68	112.7
Central Negros	6.00	0.89	13.82	2.05	53.5
Cebu Lineament	5.69	0.85	13.10	1.96	40.7
PFZ Central Leyte	5.94	0.85	13.68	1.96	72.4
Philippine Trench	7.55	1.07	17.38	2.46	202.8
Sulu Trench	7.09	1.12	16.33	2.58	30.9
Cotabato Trench	6.59	0.96	15.17	2.21	76.9

Davao River, PFZ Lianga, PFZ Eastern Mindanao, Philippine Trench and Sulu Trench. However, for seismic sources PFZ Mati, Tangbunan, MF Daguma, Lanao, MF Western Mindanao Extension, Zamboanga, East Bohol, Central Negros, Cebu Lineament and PFZ Central Leyte, large moment magnitudes earthquakes were prevailing over smaller ones since their b-values are less than 1.0.

On the other hand, the mean annual rate of occurrence ( $\lambda_{\alpha,\beta,M_0,M_{max}}$ ) of the Philippine Trench was very high at 202.8 events per year followed by PFZ Mati, PFZ Eastern Mindanao, East Bohol, Tangbunan, MF Daguma and PFZ Lianga at 147.9, 138.0, 112.7, 111.4, 110.4 and 107.6, respectively. In addition, Cotabato Trench, PFZ Central Leyte, Davao, Central Negros, Cebu Lineament, MF Western Mindanao, Sulu Trench, Lanao, Tagoloan, Cabanglasan and Zamboanga had mean annual rate of occurrences at 76.9, 72.4, 58.1, 53.5, 47.9, 40.7, 33.4, 30.9, 27.7, 18.9, 17.5 and 10.1, respectively.

### 3.3 Completeness Analysis of Earthquake Catalogue

The completeness analysis of earthquake catalog was analyzed using Stepp and CUVI methods. The number of earthquake moment magnitudes in every magnitude range from 1907 to 2018 are listed in Table 4.

Table 4. Number of earthquake events in every moment magnitude range

Magnitude Range	Number of Moment Magnitude Earthquakes
4.0-5.0	3985
5.1-6.0	2612
6.1-7.0	175
7.1 and above	32
Total	6804

In Table 4, the magnitude range of 4.0-5.0 had the most number of moment magnitude earthquake events of 3,985 events followed by the 5.1-6.0 magnitude range of 2,612 events. On the other hand, the 6.1-7.0 and 7.1-and-above had moment magnitude earthquake events of 175 and 32, respectively. The total for all magnitude ranges was 6,804 moment magnitude earthquake events.

Using the Stepp method, the values for earthquake occurrence ( $\lambda$ ) for different magnitude range and time interval based on the de-clustered catalog are calculated using Equation 3 as shown in Table 5. The N events in every magnitude range and decade are directly taken from Equation 5 or the earthquake catalog from 1907 to 2018.

Table 5. Rate of earthquake occurrence for different magnitude range and time interval based on de-clustered earthquake moment magnitudes

Period			Time T (in years)		Moment Magnitudes ( $M_w$ )					
					4.0 - 5.0		5.1 - 6.0		6.1 - 7.0	
			N	$\lambda$	N	$\lambda$	N	$\lambda$	N	$\lambda$
2011	2018	8	1202	150.3	503	62.9	31	3.9	2	0.3
2001	2018	18	2186	121.4	1177	65.4	52	2.9	6	0.3
1991	2018	28	3285	117.3	1835	65.5	73	2.6	10	0.4
1981	2018	38	3708	97.6	2127	56.0	88	2.3	13	0.3
1971	2018	48	3920	81.7	2461	51.3	111	2.3	14	0.3
1961	2018	58	3983	68.7	2586	44.6	127	2.2	15	0.3
1951	2018	68	3983	58.6	2599	38.2	138	2.0	18	0.3
1941	2018	78	3983	51.1	2602	33.4	144	1.8	20	0.3
1931	2018	88	3985	45.3	2611	29.7	152	1.7	22	0.3
1921	2018	98	3985	40.7	2612	26.7	168	1.7	28	0.3
1911	2018	108	3985	36.9	2612	24.2	174	1.6	32	0.3
1907	2018	112	3985	35.6	2612	23.3	175	1.6	32	0.3

In Table 5, the mean annual rate of occurrence ( $\lambda$ ) was computed using Equation 4 in every decade for all magnitude range. The moment magnitude range of 4.0-5.0 was occurring more often than other moment magnitude ranges of 5.1-6.0, 6.1-7.0 and 7.1-and-above as indicated by their  $\lambda$  values. For magnitude range of 4.0-5.0, there was an increase in mean annual rate of occurrences  $\lambda$ , i.e., from 35.6 of year 1907-2018 to 36.9, 40.7, 45.3, 51.1, 58.6, 68.7, 81.7, 97.6, 117.3, 121.4 and 150.3 per year of years 1911-2018, 1921-2018, 1931-2018, 1941-2018, 1951-2018, 1961-2018, 1971-2018, 1981-2018, 1991-2018, 2001-2018 and 2011-2018, respectively, indicating more earthquake events were happening recently than the previous years. The same was also happening for other magnitude ranges except for 7.1-and-above where it was almost on an even keel. The standard deviation ( $\sigma_\lambda$ ) was then calculated using the formula  $\sigma_\lambda = \frac{1}{\sqrt{T}}$ .

Table 6. Values of the standard deviation

Period			Moment Magnitudes ( $M_w$ )							
			4.0 - 5.0		5.1 - 6.0		6.1 - 7.0		7.1 and Above	
			$\lambda$	$\sigma_\lambda$	$\lambda$	$\sigma_\lambda$	$\lambda$	$\sigma_\lambda$	$\lambda$	$\sigma_\lambda$
2011	2018	8	150.3	4.33	62.9	2.80	3.9	0.70	0.3	0.18
2001	2018	18	121.4	2.60	65.4	1.91	2.9	0.40	0.3	0.14
1991	2018	28	117.3	2.05	65.5	1.53	2.6	0.31	0.4	0.11
1981	2018	38	97.6	1.60	56.0	1.21	2.3	0.25	0.3	0.09
1971	2018	48	81.7	1.30	51.3	1.03	2.3	0.22	0.3	0.08
1961	2018	58	68.7	1.09	44.6	0.88	2.2	0.19	0.3	0.07
1951	2018	68	58.6	0.93	38.2	0.75	2.0	0.17	0.3	0.06
1941	2018	78	51.1	0.81	33.4	0.65	1.8	0.15	0.3	0.06
1931	2018	88	45.3	0.72	29.7	0.58	1.7	0.14	0.3	0.05
1921	2018	98	40.7	0.64	26.7	0.52	1.7	0.13	0.3	0.05
1911	2018	108	36.9	0.58	24.2	0.47	1.6	0.12	0.3	0.05
1907	2018	112	35.6	0.56	23.3	0.46	1.6	0.12	0.3	0.05

As shown in Table 6, for the magnitude range of 4.0-5.0, it is evident that earthquake events were very close to the mean during the years 1907-2018, 1911-2018, 1921-2018, 1931-2018, 1941-2018 and 1951-2018 with less than 1.0 standard deviation ( $\sigma_\lambda$ ) values. On the contrary, earthquake events were spread out during the years 1961-2018, 1971-2018, 1981-2018, 1991-2018, 2001-2018 and 2011-2018 with more than 1.0 standard deviation ( $\sigma_\lambda$ ) values. Moreover, for the magnitude range of 5.1-6.0, earthquake events were very close to the mean during the years 1907-2018, 1911-2018, 1921-2018, 1931-2018, 1941-2018, 1951-2018, 1961-2018 and 1971-2018; they were spread out during the years 1981-2018, 1991-2018, 2001-2018 and 2011-2018. Further, earthquake events were very close to the mean for magnitude ranges of 6.1-7.0 and 7.1-and-above in all year ranges from 1907-2018 to 2011-2018.

Calculated values of the time T (in years) and the standard deviation  $\sigma_\lambda$  were plotted for a complete analysis of all earthquake moment magnitude ranges as shown in Figure 4.

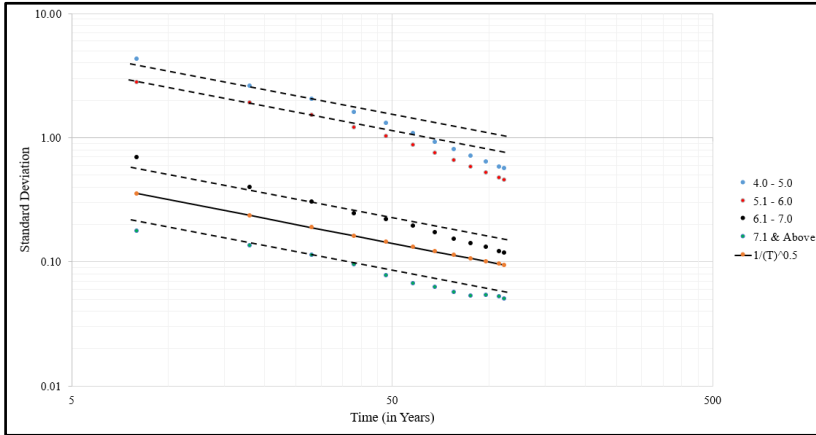


Figure 4. Completeness analysis using Stepp method

In Figure 4, the tangent line is the slope  $\frac{1}{\sqrt{T}}$ . In the magnitude range 4.0-5.0, the mean recurrence rate  $\lambda$  deviates from the tangent line from 1991-2018, i.e., the catalog is complete for 28 years. The same is true for the magnitude ranges 5.0-6.0, 6.1-7.0 and 7.1-and-above; the mean recurrence rate  $\lambda$  deviates from the tangent line from 1991-2018 where the catalog is complete also for 28 years. The other method for completeness of the earthquake catalog is the CUVI method as shown in Figure 5.

In Figure 5a-5d, the completeness period for earthquake magnitude ranges 4.0-5.0, 5.1-6.0, 6.1-7.0 and 7.1-and-above using polynomial regression is 28 years (1991-2018). Table 7 shows the completeness period of the study area using Stepp and CUVI methods.

### 3.4 Earthquake Seismic Sources and Magnitudes

Using Equations 6 and 7, the CDF was calculated. The results are summarized in Table 8.

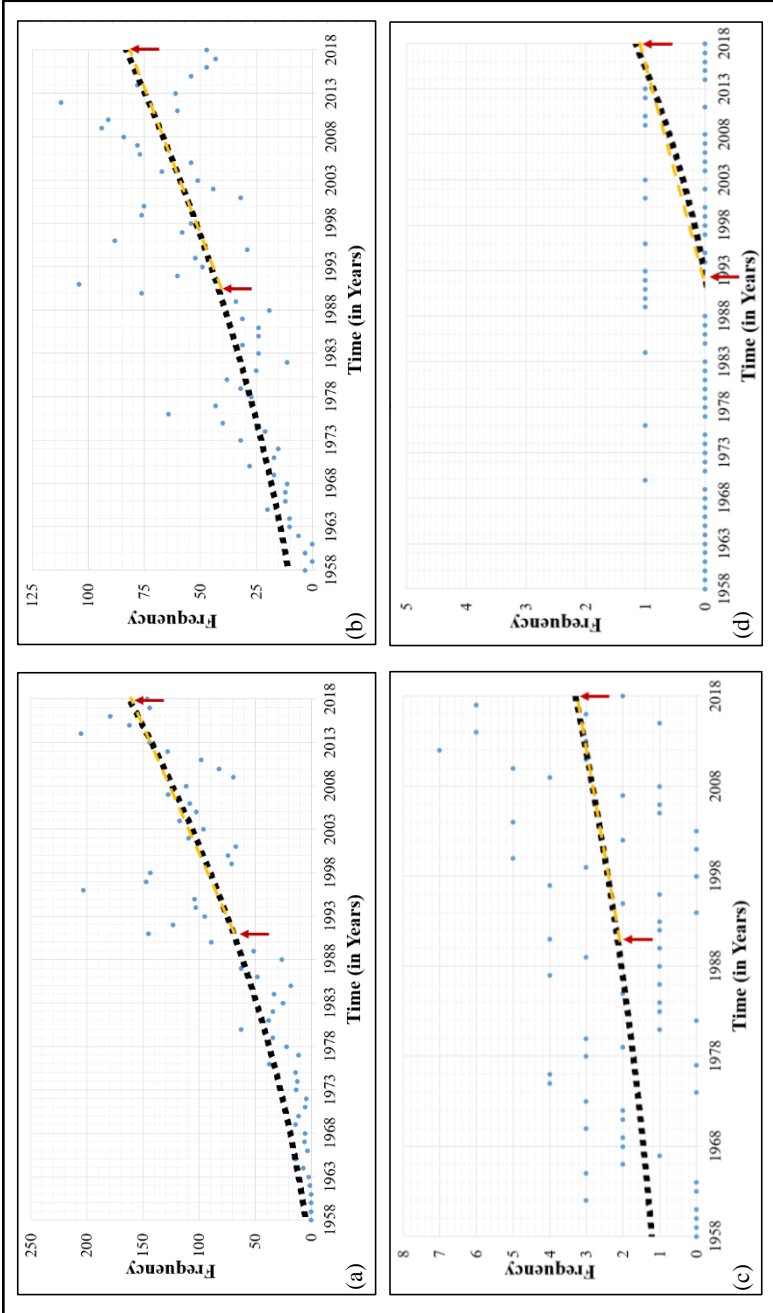


Figure 5. Completeness periods for magnitude range: 4.0-5.0 (a), 5.1-6.0 (b), 6.1-7.0 (c) and 7.1 and above (d)

Table 7. Completeness period of the study area

Moment Magnitude Interval ( $M_w$ )	Completeness Period	Number of Years	
		STEPP Method	CUVI Method
4.0 - 5.0	1991 - 2018	28	28
5.1 - 6.0	1991 - 2018	28	28
6.1 - 7.0	1991 - 2018	28	28
7.1 and above	1991 - 2018	28	28

Table 8. Calculated CDF for all seismic sources

Seismic Source	CDF of $M_w$						
	5.0	5.5	6.0	6.5	7.0	7.5	8.0
Tagoloan River	0.0000	0.5845	0.9323	1.0000	1.0000	1.0000	1.0000
Cabanglasan	0.0000	0.7335	0.9634	1.0000	1.0000	1.0000	1.0000
Central Mindanao	0.0000	0.7146	0.9207	0.9801	0.9973	1.0000	1.0000
Davao River	0.2144	0.7673	0.9343	0.9848	1.0000	1.0000	1.0000
PFZ Mati	0.0000	0.6735	0.8939	0.9661	0.9897	0.9975	1.0000
PFZ Lianga	0.0000	0.6928	0.9301	0.9845	0.9969	0.9998	1.0000
PFZ East. Mindanao	0.0000	0.7087	0.9155	0.9758	0.9934	0.9985	1.0000
Tangbunan	0.2011	0.7417	0.9186	0.9765	0.9955	1.0000	1.0000
MF Daguma	0.1750	0.6863	0.8829	0.9585	0.9876	0.9988	1.0000
Lanao	0.0000	0.3419	0.7746	0.9299	0.9857	1.0000	1.0000
MF West. Mindanao	0.0000	0.5529	0.8406	0.9474	0.9872	1.0000	1.0000
Zamboanga	0.0000	0.3710	0.8079	0.9476	0.9923	1.0000	1.0000
East Bohol	0.4958	0.7897	0.9165	0.9713	0.9949	1.0000	1.0000
Central Negros	0.3400	0.7703	0.9247	0.9801	1.0000	1.0000	1.0000
Cebu Lineament	0.3276	0.7543	0.9146	0.9749	0.9976	1.0000	1.0000
PFZ Central Leyte	0.3283	0.7561	0.9169	0.9773	1.0000	1.0000	1.0000
Phil. Trench	0.2187	0.7730	0.9347	0.9819	0.9956	0.9996	1.0000
Sulu Trench	0.0000	0.7509	0.9577	1.0000	1.0000	1.0000	1.0000
Cotabato Trench	0.1988	0.7364	0.9144	0.9734	0.9929	0.9994	1.0000

Based on Table 8, the CDF, which is a probabilistic tool used to determine the probability of a certain moment magnitude earthquake  $M_w$  to occur in a seismic source, was calculated using Equation 7. For all seismic sources, the greater is the value of the CDF of a certain  $M_w$ , the lesser is the probability of occurrence of such  $M_w$  and vice-versa. For the Tagoloan river fault at  $M_w = 5.5$ , the CDF is 0.5845 while for  $M_w = 6.0$ , the CDF is 0.9323. Thus, an earthquake with a moment magnitude  $M_w$  of 5.5 has the greater probability of occurring than the  $M_w$  of 6.0. Using the calculated values of CDF in Table 8, the probability that  $M_w$  is equal to  $m_i$  was calculated using Equation 8. The probabilities of certain earthquake moment magnitude  $M_w$  occurring at each seismic source as shown in Table 9.

Table 9. Probabilities of moment magnitude  $M_w$  equal to  $M_i$  for all seismic sources

Seismic Source	5.0	5.5	6.0	6.5	7.0	7.5	8.0
Tagoloan River	0.2490	0.0013	0.0003	0.0000	0.0000	0.0000	0.0000
Cabanglasan	0.2768	0.0784	0.0162	0.0000	0.0000	0.0000	0.0000
Central Mindanao	0.2211	0.0638	0.0184	0.0053	0.0015	0.0000	0.0000
Davao River	0.1687	0.0509	0.0154	0.0046	0.0000	0.0000	0.0000
PFZ Mati	0.2004	0.0656	0.0215	0.0070	0.0023	0.0008	0.0000
PFZ Lianga	0.2554	0.0786	0.0180	0.0041	0.0009	0.0002	0.0000
PFZ East. Mindanao	0.2185	0.0637	0.0186	0.0054	0.0016	0.0005	0.0000
Tangbulan	0.1609	0.0527	0.0172	0.0056	0.0018	0.0000	0.0000
MF Daguma	0.1750	0.0556	0.0214	0.0082	0.0032	0.0012	0.0000
Lanao	0.1184	0.1251	0.0449	0.0161	0.0058	0.0000	0.0000
MF West. Mindanao	0.1816	0.0822	0.0306	0.0114	0.0042	0.0000	0.0000
Zamboanga	0.2066	0.1309	0.0419	0.0134	0.0043	0.0000	0.0000
East Bohol	0.0800	0.0345	0.0149	0.0064	0.0028	0.0000	0.0000
Central Negros	0.1244	0.0446	0.0160	0.0058	0.0000	0.0000	0.0000
Cebu Lineament	0.1215	0.0457	0.0172	0.0065	0.0024	0.0000	0.0000
PFZ Central Leyte	0.1218	0.0458	0.0172	0.0065	0.0000	0.0000	0.0000
Phil. Trench	0.1709	0.0499	0.0145	0.0042	0.0012	0.0004	0.0000
Sulu Trench	0.2356	0.0649	0.0179	0.0000	0.0000	0.0000	0.0000
Cotabato Trench	0.1594	0.0528	0.0175	0.0058	0.0019	0.0006	0.0000

In Table 9, moment magnitudes  $M_w$  of 5.0, 5.5 and 6.0 at the Tagoloan River Fault have probabilities of occurrence at 24.9, 0.13 and 0.03% while for  $M_w$  of 6.5, 7.0, 7.5 and 8.0, there is no probability of occurrence. For the Cabanglasan Fault,  $M_w$  of 5.0, 5.5 and 6.0 have probabilities of occurrence at 27.68, 7.84 and 1.62% while for  $M_w$  of 6.5, 7.0, 7.5 and 8.0, there is no probability of occurrence.

For Central Mindanao Fault,  $M_w$  of 5.0, 5.5, 6.0, 6.5 and 7.0 have probability of occurrence at 22.11, 6.38, 1.84, 0.53 and 0.15%, respectively, while  $M_w$  of 7.5 and 8.0 have no probabilities of occurrence. For the Davao River Fault,  $M_w$  of 5.0, 5.5, 6.0 and 6.5 have probabilities of occurrence at 16.87, 5.09,

1.54 and 0.46%, respectively, while for  $M_w$  of 7.0, 7.5 and 8.0 have no probabilities of occurrence. The PFZ Mati Fault,  $M_w$  of 5.0, 5.5, 6.0, 6.5, 7.0, 7.5 and 8.0 have probabilities of occurrence at 20.04, 6.56, 2.15, 0.70, 0.23, 0.08 and 0.00%, respectively. The PFZ Lianga Fault,  $M_w$  of 5.0, 5.5, 6.0, 6.5, 7.0, 7.5 and 8.0 have probabilities of occurrence at 25.54, 7.86, 1.80, 0.41, 0.09, 0.02 and 0.00%, respectively. For the PFZ Eastern Mindanao Fault,  $M_w$  of 5.0, 5.5, 6.0, 6.5, 7.0, 7.5 and 8.0 have probabilities of occurrence at 21.85, 6.37, 1.86, 0.54, 0.16, 0.05 and 0.00%, respectively.

For the Tangbulan Fault,  $M_w$  of 5.0, 5.5, 6.0, 6.5 and 7.0 have probabilities of occurrence at 16.09, 5.27, 1.72, 0.56 and 0.18%, respectively, while  $M_w$  of 7.5 and 8.0 have no probabilities of occurrence at all. For MF Daguma Extension Fault,  $M_w$  of 5.0, 5.5, 6.0, 6.5, 7.0, 7.5 and 8.0 have probabilities of occurrence at 17.50, 5.56, 2.14, 0.82, 0.32, 0.12 and 0.00%, respectively. For the Lanao Fault,  $M_w$  of 5.0, 5.5, 6.0, 6.5 and 7.0 have probabilities of occurrence at 11.84, 12.51, 4.49, 1.61 and 0.58% while  $M_w$  of 7.5 and 8.0 have no probabilities of occurrence at all. For the MF Western Mindanao Fault,  $M_w$  of 5.0, 5.5, 6.0, 6.5 and 7.0 have probabilities of occurrence at 18.16, 8.22, 3.06, 1.14 and 0.42%, respectively, while  $M_w$  of 7.5 and 8.0 have no probabilities of occurrence. For the Zamboanga Fault,  $M_w$  of 5.0, 5.5, 6.0, 6.5 and 7.0 have probabilities of occurrence at 20.66, 13.09, 4.19, 1.34 and 0.43%, respectively, while  $M_w$  of 7.5 and 8.0 have no probabilities of occurrence.

For the East Bohol Fault,  $M_w$  of 5.0, 5.5, 6.0, 6.5 and 7.0 have probabilities of occurrence at 8.00, 3.45, 1.49, 0.64 and 0.28%, respectively, while  $M_w$  of 7.5 and 8.0 have no probabilities of occurrence. For the Central Negros, Cebu Lineament and PFZ Central Leyte Faults,  $M_w$  of 5.0, 5.5, 6.0 and 6.5 have probabilities of occurrence at about 12.00, 5.00, 2.00 and 1.00%, respectively while  $M_w$  of 7.0, 7.5 and 8.0 have no probabilities of occurrence. For the Philippine Trench,  $M_w$  of 5.0, 5.5, 6.0, 6.5 and 7.0 have probabilities of occurrence at 17.09, 4.99, 1.45, 0.42 and 0.12%, respectively, while  $M_w$  of 7.5 and 8.0 have no probabilities of occurrence. For the Sulu Trench,  $M_w$  of 5.0, 5.5 and 6.0 have probabilities of occurrence at 23.56, 6.49 and 1.79%, respectively, while  $M_w$  of 6.5, 7.0, 7.5 and 8.0 have no probabilities of occurrence. Finally, for the Cotabato Trench,  $M_w$  of 5.0, 5.5, 6.0, 6.5 and 7.0 have probabilities of occurrence at 15.94, 5.28, 1.75, 0.58 and 0.19%, respectively, while  $M_w$  of 7.5 and 8.0 have no probabilities of occurrence at all.

### 3.5 Shear Wave Velocities ( $V_{s30}$ )

From the geotechnical soil test reports, SPT-N values of 95 boreholes were correlated using Equation 9 to get shear-wave velocities at different depths for alluvial soils. Consequently, Equation 10 was used to predict average upper 30-meter shear-wave velocities ( $V_{s30}$ ) of different soils. Finally, using the Empirical Bayesian Kriging Method of the ArcGIS software, a .tiff file was created and converted to .grd file in Surfer software for  $V_{s30}$  values as shown in Table 10.

Table 10.  $V_{s30}$  values in the 2<sup>nd</sup> district of Cagayan de Oro City, Philippines

Sites	$V_{s30}$ (m/s)	Sites	$V_{s30}$ (m/s)
Agusan	383	Barangay 13	366
Balubal	401	Barangay 14	364
Bugo	394	Barangay 15	367
Camaman-an	389	Barangay 16	363
Consolacion	360	Barangay 17	367
Cugman	404	Barangay 18	364
FS Catanico	403	Barangay 19	362
Gusa	411	Barangay 20	360
Indahag	389	Barangay 21	353
Lapasan	372	Barangay 22	341
Macabalan	357	Barangay 23	354
Macasandig	396	Barangay 24	344
Nazareth	371	Barangay 25	355
Puerto	403	Barangay 26	343
Puntod	354	Barangay 27	357
Tablon	381	Barangay 28	350
Barangay 1	368	Barangay 29	363
Barangay 2	368	Barangay 30	358
Barangay 3	364	Barangay 31	351
Barangay 4	366	Barangay 32	359
Barangay 5	366	Barangay 33	358
Barangay 6	368	Barangay 34	357
Barangay 7	367	Barangay 35	359
Barangay 8	365	Barangay 36	362
Barangay 9	362	Barangay 37	362
Barangay 10	367	Barangay 38	363
Barangay 11	364	Barangay 39	361
Barangay 12	365	Barangay 40	364

Gusa had the highest shear-wave velocity value at 411 m/s followed by Cugman, FS Catanico, Puerto and Balubal at 404, 403 and 401 m/s, respectively. This was followed by Macasandig (396 m/s), Bugo (394 m/s), Indahag/Camaman-an (389 m/s), Agusan (383 m/s), Tablon (381 m/s), Lapasan (372 m/s) and Nazareth (371 m/s). On the other hand, Consolacion, Barangays 1-20, Barangay 29 and Barangay 36-40 had  $V_{s30}$  values ranging from 360 to 368 m/s and the rest had values ranging from 341 to 359 m/s.

These values were then exported to the R-CRISIS 2015 software in .grid file for local site effects consideration.

### 3.6 Site-Specific Response Spectra

The R-CRISIS 2015 software was utilized in the development of site-specific response spectra in the 2<sup>nd</sup> District of Cagayan de Oro City, Philippines. The Basic PSHA procedure conducted, using the R-CRISIS software, is shown in Figures 6-10.

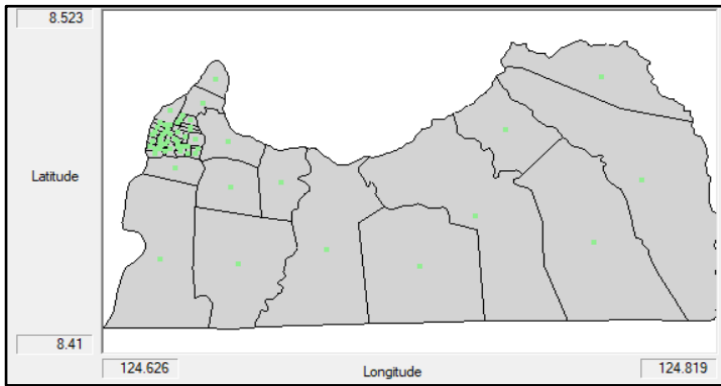


Figure 6. Map and city files

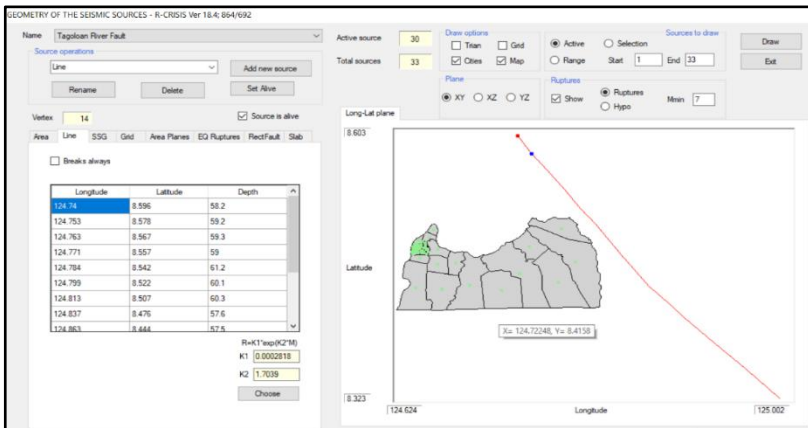


Figure 7. Seismic source geometry

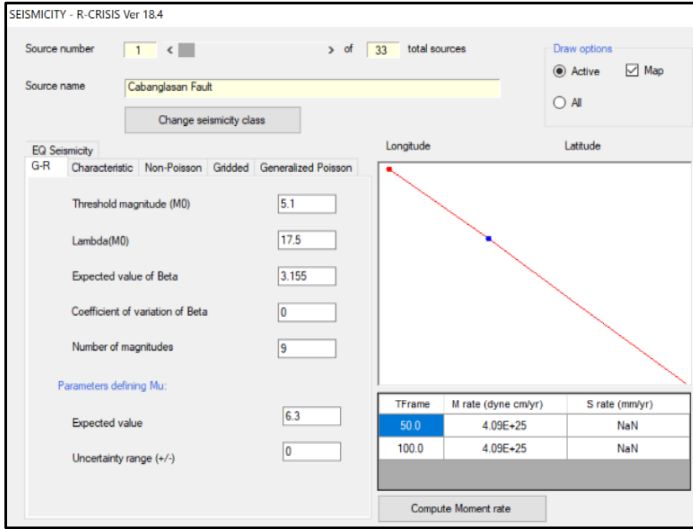


Figure 8. Seismicity of the study area

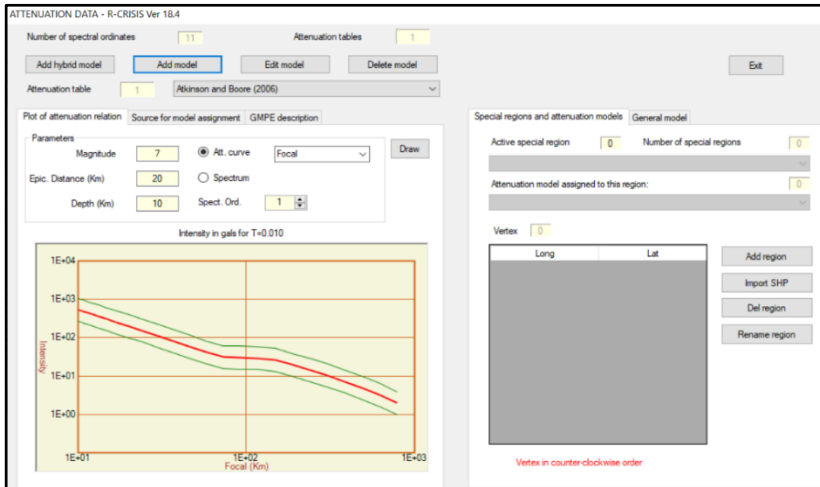


Figure 9. Attenuation equation or ground motion prediction equation

Based on Figures 6 to 10, after exporting the map and city files (Figure 6), a  $0.1^\circ \times 0.1^\circ$  grid of site was used. The geometry of seismic sources was then inserted to characterize fault lines (Figure 7) consisting of 33 line seismic sources within the 300-km radius. The seismicity of the study area was then considered (Figure 8) by filling in the  $M_0$ ,  $\lambda_{\alpha,\beta,M_0}$ ,  $M_{max}$ ,  $\beta$  and  $M_{max}$ .

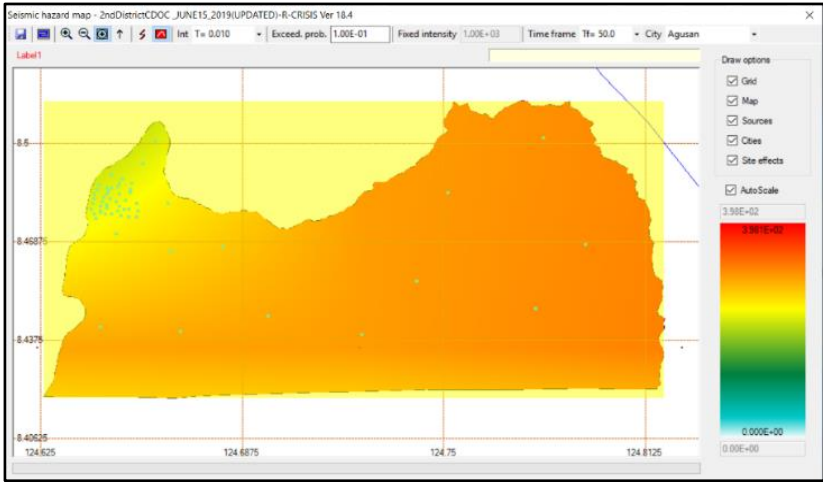


Figure 10. Site effects of local soil condition

The Atkinson and Boore (2006) GMPE or attenuation for soil sites (Figure 9) was used in the R-CRISIS 2015 software since the geologic history of the study area is an alluvial soil deposit. The  $V_{s30}$ .grd file was then transported (Figure 10) for local site effects consideration. The corresponding ground surface site-specific response spectra in the 2<sup>nd</sup> District of Cagayan de Oro City, Philippines are shown in Figure 11.

Figure 11a is the response spectrum of Balubal, Bugo and Puerto having spectral accelerations of 386 gals or 39% of gravity (0.39g) at time  $t = 0.01$  s, 904 gals (0.92 g) at  $t = 0.2$  s, 224 gals (0.23 g) at  $t = 1.0$  s, 95 gals (0.10 g) at  $t = 2.0$  s, 66 gals (0.07 g) at  $t = 3.0$  s, 51 gals (0.05 g) at  $t = 4.0$  s and 37 gals (0.04 g) at  $t = 5.0$  s, respectively.

Figure 11b is the response spectrum of Agusan and Tablon having spectral accelerations of 370 gals or 38% of gravity (0.38 g) at time  $t = 0.01$  s, 876 gals (0.89 g) at  $t = 0.2$  s, 222 gals (0.23 g) at  $t = 1.0$  s, 95 gals (0.10 g) at  $t = 2.0$  s, 65 gals (0.07 g) at  $t = 3.0$  s, 51 gals (0.05 g) at  $t = 4.0$  s and 37 gals (0.04 g) at  $t = 5.0$  s, respectively.

Figure 11c is the response spectrum of FS Catanico having spectral accelerations of 362 gals or 37% of gravity (0.37 g) at time  $t = 0.01$  s, 862 gals (0.88 g) at  $t = 0.2$  s, 221 gals (0.23 g) at  $t = 1.0$  s, 95 gals (0.10g) at  $t = 2.0$  s, 65 gals (0.07 g) at  $t = 3.0$  s, 51 gals (0.05 g) at  $t = 4.0$  s and 37 gals (0.04 g) at  $t = 5.0$  s, respectively.

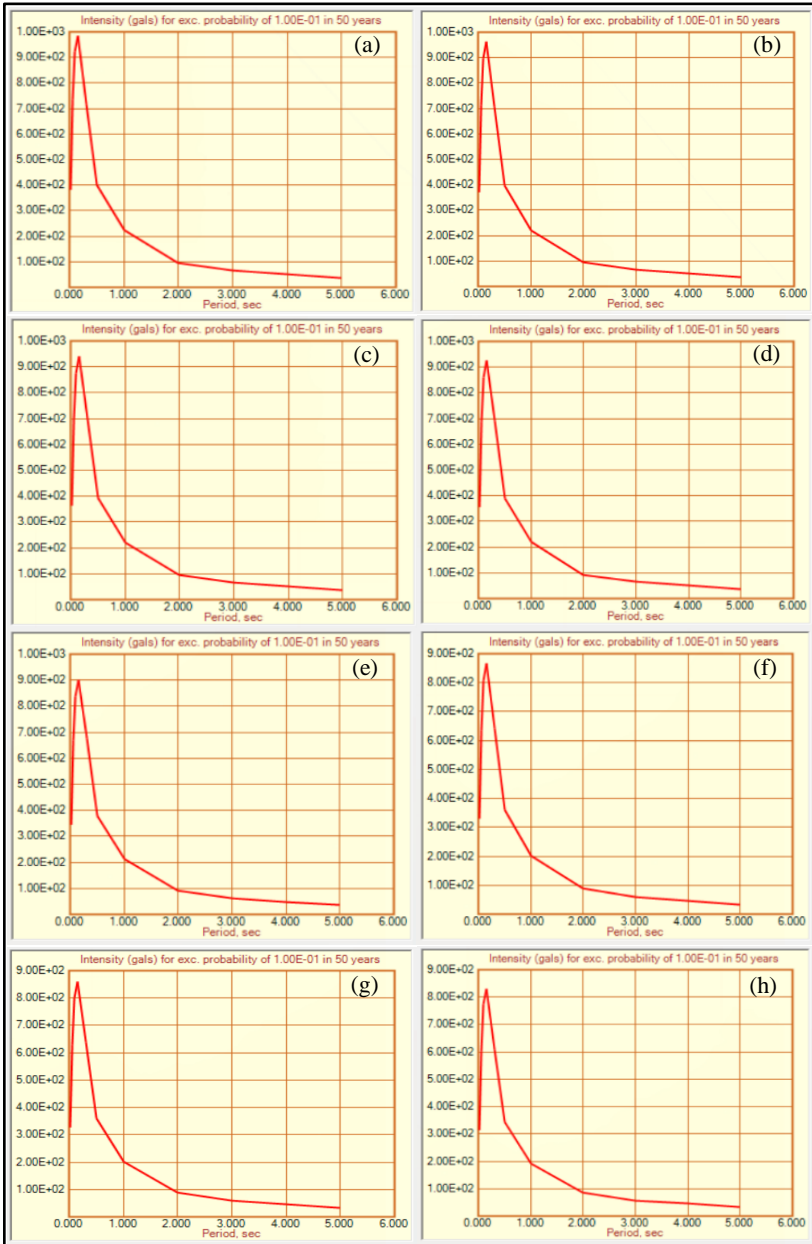


Figure 11. Site-specific response spectra of the study area – Balubal, Bugo and Puerto (a), Agusan and Tablon (b), FS Catanico (c), Cugman and Indahag (d), Camaman-an, Gusa and Macasandig (e), Lapan (f), Nazareth and Barangays 1, 3, 4, 9, 24, 26, 28, 30-40 (g) and Consolacion, Macabalan, Puntod and Barangays 2, 5-8, 10-23, 25, 27, 29 (h)

Figure 11d is the response spectrum of Cugman and Indahag having spectral accelerations of 356 gals or 36% of gravity (0.36 g) at time  $t = 0.01$  s, 848 gals (0.86 g) at  $t = 0.2$  s, 219 gals (0.22 g) at  $t = 1.0$  s, 94 gals (0.10 g) at  $t = 2.0$  s, 65 gals (0.07 g) at  $t = 3.0$  s, 50 gals (0.05 g) at  $t = 4.0$  s and 37 gals (0.04 g) at  $t = 5.0$  s, respectively.

Figure 11e is the response spectrum of Camaman-an, Gusa and Macasandig having spectral accelerations of 348 gals or 35% of gravity (0.35 g) at time  $t = 0.01$  s, 829 gals (0.85 g) at  $t = 0.2$  s, 216 gals (0.22 g) at  $t = 1.0$  s, 93 gals (0.09 g) at  $t = 2.0$  s, 64 gals (0.07 g) at  $t = 3.0$  s, 50 gals (0.05 g) at  $t = 4.0$  s and 36 gals (0.04 g) at  $t = 5.0$  s, respectively.

Figure 11f is the response spectrum of Lapasan having spectral accelerations of 329 gals or 34% of gravity (0.34 g) at time  $t = 0.01$  s, 790 gals (0.81 g) at  $t = 0.2$  s, 202 gals (0.21 g) at  $t = 1.0$  s, 88 gals (0.09 g) at  $t = 2.0$  s, 60 gals (0.06 g) at  $t = 3.0$  s, 47 gals (0.05 g) at  $t = 4.0$  s and 34 gals (0.03 g) at  $t = 5.0$  s, respectively.

Figure 11g is the response spectrum of Nazareth and Barangays 1, 3, 4, 9, 24, 26, 28, 30-40 having spectral accelerations of 327 gals or 33% of gravity (0.33 g) at time  $t = 0.01$  s, 785 gals (0.80 g) at  $t = 0.2$  s, 202 gals (0.21 g) at  $t = 1.0$  s, 88 gals (0.09 g) at  $t = 2.0$  s, 60 gals (0.06 g) at  $t = 3.0$  s, 47 gals (0.05 g) at  $t = 4.0$  s and 34 gals (0.03 g) at  $t = 5.0$  s, respectively.

Finally, Figure 11h is the response spectrum of Consolacion, Macabalan, Puntod and Barangays 2, 5-8, 10-23, 25, 27, 29 having spectral accelerations of 315 gals or 32% of gravity (0.32 g) at time  $t = 0.01$  s, 758 gals (0.77 g) at  $t = 0.2$  s, 193 gals (0.20g) at  $t = 1.0$  s, 85 gals (0.09 g) at  $t = 2.0$  s, 57 gals (0.06 g) at  $t = 3.0$  s, 45 gals (0.05 g) at  $t = 4.0$  s and 32 gals (0.03 g) at  $t = 5.0$  s, respectively. It is apparent that the UBC 1997 Code is more conservative than the ground surface site-specific response spectra in the 2<sup>nd</sup> District of Cagayan de Oro City, Philippines, which indicates building cost and design considerations. The graph of ground surface site-specific response spectra vs. the UBC-1997 is shown in Figure 12.

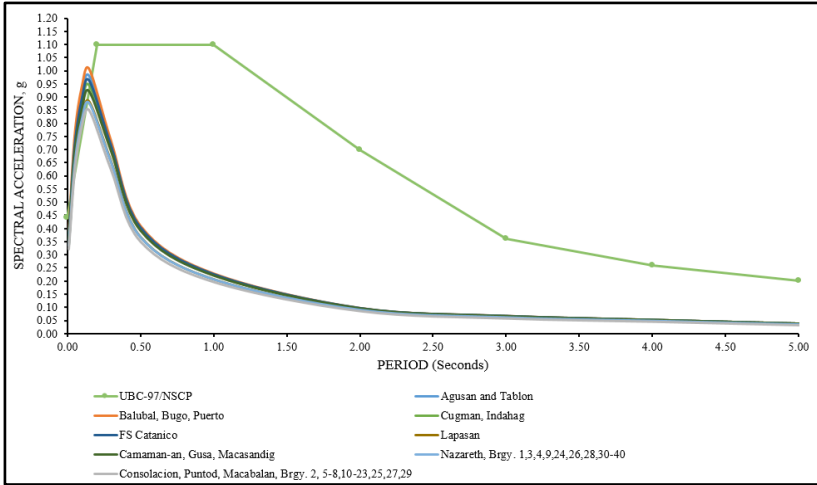


Figure 12. Site-specific response spectra in the 2<sup>nd</sup> district of Cagayan de Oro City, Philippines vs. the UBC (1997)

#### 4. Conclusion and Recommendation

Based on the results, the ground surface site-specific response spectrum of Balubal, Bugo and Puerto, which has the highest spectral acceleration of 386 gals or 39% of gravity (0.39 g) at time  $t = 0.01$  s, 904 gals (0.92 g) at  $t = 0.2$  s, 224 gals (0.23 g) at  $t = 1.0$  s, 95 gals (0.10 g) at  $t = 2.0$  s, 66 gals (0.07 g) at  $t = 3.0$  s, 51 gals (0.05 g) at  $t = 4.0$  s and 37 gals (0.04 g) at  $t = 5.0$  s, respectively. These are way below the UBC 1997 Code of 432 gals or 44% of gravity (0.44 g) at time  $t = 0.00$  s, 1079 gals (1.10g) at  $t = 0.2$  s, 1079 gals (1.10 g) at  $t = 1.0$  s, 687 gals (0.70 g) at  $t = 2.0$  s, 353 gals (0.36 g) at  $t = 3.0$  s, 255 gals (0.26g) at  $t = 4.0$  s and 196 gals (0.20 g) at  $t = 5.0$  s. It is therefore concluded that site-specific response spectra in the 2<sup>nd</sup> District of Cagayan de Oro City, Philippines is a doable alternative in the design of building structures.

In line with the conclusion made, it is recommended to use the ground surface site-specific response spectra in the 2<sup>nd</sup> District of Cagayan de Oro City, Philippines for future building constructions. Site-specific response spectra can be used by building owners, both private and government entities, in the design of future building structures where they can save economically while maintaining the structural integrity and stability of the building against future earthquakes.

## **5. References**

- Ahmad, N. (2016). Steps for conducting probabilistic seismic hazard analysis using GIS and CRISIS tools (Technical Report). University of Engineering and Technology, Peshawar.
- Akin, M., Kramer, S.L., & Topal, T. (2011). Empirical correlations of shear wave velocity ( $V_s$ ) and penetration resistance (SPT-N) for different soils in an earthquake-prone area (Erbaa-Turkey). *Engineering Geology*, 119(1-2), 1-17. <https://doi.org/10.1016/j.enggeo.2011.01.007>
- Anbazhagan, P., Bajaj, K., Dutta, N., Moustafa, S.S.R., & Al-Arifi, N.S.N. (2016). Region-specific deterministic and probabilistic seismic hazard analysis of Kanpur City. *Journal of Earth System Science*, 126, 12. <https://doi.org/10.1007/s12040-016-0779-6>
- Atkinson, G.M., and Boore, D.M. (2006). Earthquake ground-motion prediction equations for Eastern North America. *Bulletin of the Seismological Society of America*, 96(6), 2181-2205. <https://doi.org/10.1785/0120050245>
- Association of Structural Engineers of the Philippines. (2015). National Structural Code of the Philippines (7<sup>th</sup> Ed., Vol. 1). Quezon City, Philippines: Association of Structural Engineers of the Philippines, Inc.
- Boore, D.M., Thompson, E.M., & Cadet, H. (2011). Regional correlations of  $V_{S30}$  and velocities averaged over depths less than and greater than 30 meters. *Bulletin of the Seismological Society of America*, 101(6), 3046-3059. <https://doi.org/10.1785/0120110071>
- Cagayan de Oro City Planning and Development Office. (2015). Socio-Economic Profile. Retrieved from <http://www.cagayandeoro.gov.ph/about-cdo/economic>
- Dungca, J., & Macaraeg, C. (2016). Integration of site effects to probabilistic seismic hazard analysis for estimation of peak ground acceleration. *Proceedings of 6<sup>th</sup> ASIA Conference on Earthquake Engineering (6A CEE)*, Cebu City, Philippines, 1-11.
- Ordaz, M., & Salgado-Galvez, M.A. (2017). R-CRISIS validation and verification document (ERN Technical Report). Mexico City, Mexico: Instituto de Ingeniería – Universidad Nacional Autónoma de México & Evaluación de Riesgos Naturales.
- Salamat, M., & Zare, M. (2015). Application of stepp method for assessing the completeness of instrumental and pre-instrumental earthquake data in different seismic provinces of Iran. *Proceedings of 7<sup>th</sup> International Conference on Seismology & Earthquake Engineering*, Tehran, Iran, 215-216.
- Sil, A., & Sitharam, T.G. (2016). Site-specific design response spectrum proposed for the Capital City of Agartala, Tripura. *Geomatics, Natural Hazards and Risk*, 7(5), 1610-1630. <https://doi.org/10.1080/19475705.2015.1124929>
- Stepp, J.C. (2001). Analysis of completeness of the earthquake sample in the Puget Sound area and its effect on statistical estimates of earthquake hazard. *Proceedings of the International Conference on Microzonation*, Seattle, USA, 897-910.
- Teng, G., & Baker, J.W. (2019). Seismicity declustering and hazard analysis of the Oklahoma-Kansas region. *Bulletin of the Seismological Society of America*, 109(6), 2356-2366. <https://doi.org/10.1785/0120190111>